Journal of the European Ceramic Society xxx (xxxx) xxx–xxx

Contents lists available at ScienceDirect

Journal of the European Ceramic Society

journal homepage: www.elsevier.com/locate/jeurceramsoc

Original Article

Li_2AGeO_4 (A = Zn, Mg): Two novel low-permittivity microwave dielectric ceramics with olivine structure

Chunchun Li[a,b,*], Huaicheng Xiang[a], Minyu Xu[a], Ying Tang[a], Liang Fang[a,*]

[a] State Key Laboratory Breeding Base of Nonferrous Metals and Specific Materials Processing, Guangxi Universities Key Laboratory of Non-Ferrous Metal Oxide Electronic Functional Materials and Devices, College of Material Science and Engineering, Guilin University of Technology, Guilin, 541004, China
[b] College of Information Science and Engineering, Guilin University of Technology, Guilin, 541004, China

ARTICLE INFO

Keywords:
Dielectric properties
Millimeter wave
Low permittivity
Olivine structure

ABSTRACT

Two low-permittivity dielectric materials Li_2AGeO_4 (A = Zn, Mg) were prepared via the solid-state reaction method. X-ray diffraction analysis and Rietveld refinement indicated that both ceramics crystallize in an orthorhombic olivine structure with a space group *Pmn2₁*. Dense ceramics with high relative density and homogeneous microstructure were obtained. Li_2ZnGeO_4 densified at 1200 °C possessed a relative permittivity ε_r = 6.5, a quality factor $Q \times f$ = 35,400 GHz, and a temperature coefficient of resonant frequency. Li_2MgGeO_4 exhibited ε_r = 6.1, $Q \times f$ = 28,500 GHz, and τ_f = –74.7 ppm/°C when sintered at 1220 °C. Additionally, the large negative τ_f values of Li_2AGeO_4 (A = Zn, Mg) ceramics were successfully adjusted compensated by forming composite ceramics with $CaTiO_3$ and near-zero τ_f values of +2.9 ppm/°C and +5.8 ppm/°C were achieved in $0.92Li_2ZnGeO_4$-$0.08CaTiO_3$ and $0.90Li_2MgGeO_4$-$0.10CaTiO_3$, respectively.

1. Introduction

The rapid advance in wireless communications to millimeter waves such as electronic transport cashing (ETC), ultra-high speed LAN, car anti-collision system on the intelligent transport system (ITS), in recent years, has triggered tremendous development in microwave dielectrics. In millimeter-wave applications, a large number of information can be transferred at a high speed [1–4]. Thus, three primary figures of merit are required: low permittivity (ε_r), high quality factor (low dielectric loss, $Q = 1/\tan\delta$), and near-zero temperature coefficient of resonant frequency (τ_f) [5,6]. Importantly, the signal delay time is proportional to the square root of permittivity according to the formula $t_d = \sqrt{\varepsilon_r} l_e/c$ (where t_d, l_e, and c represents signal delay time, transmission distance, and velocity of light) [7]. Thus, low ε_r is desirable for high-speed transmission. Additionally, low permittivity also minimizes the cross-coupling between the substrates with the conductors and decreases the latency in long-range reception. Therefore, the development of low-permittivity microwave dielectric materials to cater high-speed transmission demands is becoming a hot issue.

In the past several decades, numerous low-ε_r materials, such as Al_2O_3, spinel MAl_2O_4 and M_2TiO_4 (M = Mg, Zn), and forsterite M_2SiO_4 (M = Mg, Zn), have been developed for millimeter-wave applications [8–14]. For example, Mg_2SiO_4 ceramics sintered at 1550 °C possessed excellent microwave dielectric performance with ε_r = 7.50, $Q \times f$ = 114,730 GHz, and τ_f = –59 ppm/°C [13]. The olivine structure has a general formula A_2BO_4, in which B^{4+} locates at the center of isolated tetrahedral geometry. Compared with spinel structure AB_2O_4, where A ions, usually divalent, are coordinated by four oxygen ions forming AO_4 tetrahedral, while B ions, usually trivalent, are coordinated by six oxygen ions forming BO_6 octahedral. Substitution of two trivalent B ions in the spinel AB_2O_4 by one divalent A and one tetravalent ion will result in an inverse spinel structure, such as Mg[MgTi]O_4 [15,16,17]. More recently, considerable attention has been focused on the M_2GeO_4 (M = Mg, Zn) olivine compounds due to their low permittivity and high quality factor [18–20]. For example, orthorhombic Mg_2GeO_4 ceramic sintered at 1450 °C had a low permittivity $\varepsilon_r \sim$ 5.48, a quality factor $Q \times f \sim$ 11,037 GHz, and a temperature coefficient of resonant frequency $\tau_f \sim$ –27.61 ppm/°C [19]. Nevertheless, these low permittivity microwave dielectric ceramics generally have high sintering temperatures and negative large τ_f values, which are undesirable for practical applications. In recent years, Li-containing oxides have been reported as low-firing ceramics, e.g. $Li_4Ti_5O_{12}$ [21], $Li_2ZnTi_3O_8$ [22], and $Li_2ZnGe_3O_8$ [23]. Therefore, it is possible to reduce the sintering temperature of M_2GeO_4 by introducing Li^+ ionic into the olivine structure. Therefore, in the parent M_2GeO_4, we introduced 2 Li^+ ions to substitute 1 M cation to synthesize two olivine Li_2MGeO_4 (M = Zn, Mg) ceramics with structure. And their microwave dielectric properties were characterized for the first time. In

* Corresponding author.
E-mail addresses: lichunchun2003@126.com (H. Xiang), fanglianggl001@aliyun.com (L. Fang).

https://doi.org/10.1016/j.jeurceramsoc.2017.12.038
Received 11 October 2017; Received in revised form 17 December 2017; Accepted 18 December 2017

addition, $CaTiO_3$ ($\tau_f \sim +800$ ppm/°C) was utilized to form composite ceramics with Li_2MGeO_4 to obtain thermally stable dielectric materials.

2. Experimental procedure

The Li_2AGeO_4 (A = Zn, Mg) ceramics were prepared by solid-state reaction of Li_2CO_3 (99.99%, Guo-Yao Co. Ltd., China), ZnO (99.99%, Guo-Yao Co. Ltd., China), MgO (99.99%, Guo-Yao Co. Ltd., China), and GeO_2 (99.999%, Guo-Yao Co. Ltd., China) as starting materials. Importantly, MgO powers were heated at 900 °C for 1 h to remove moisture. The starting materials were weighed according to the stoichiometry and mixed through ball milling using ZrO_2 balls with ethanol as the medium for 6 h. The dried mixtures were calcined at 1100 °C for 6 h in a platinum crucible, and re-milled for 4 h. Then PVA was added as binder, ground and pressed into 10 mm-diameter and 6 mm-height disks under a pressure of 350 MPa. The green compacts were firstly fired at 550 °C in air for 2 h to expel the organic binder and then sintered at 1140 °C–1240 °C for 6 h.

The crystal structure and phase purity were examined by powder X-ray diffraction (XRD) which was performed on a Panalytical X'Pert PRO diffractometer with Cu Kα radiation. The surface microstructures of the pellets were observed by a Hitachi (Tokyo, Japan) S4800 scanning electron microscopy (SEM). The densities of the sintered ceramics were measured using the Archimedes' method. The permittivity and quality factor values were measured in the TE_{011} mode according to the Hakki-Coleman method using an Agilent N5230A network analyzer (Palo Alto, CA). The temperature coefficient of resonate frequency τ_f value was measured from 25 °C to 85 °C using a temperature chamber (Delta 9039, Delta Design, San Diego, CA).

3. Results and discussion

Fig. 1 shows the Rietveld refinements using Fullprof software were performed on the XRD data of Li_2ZnGeO_4 and Li_2MgGeO_4 and the calculated and measured diffraction patterns along with the unit cell volume and the schematic crystal structure. The consistent match between the calculated and measured diffraction patterns and the low residual factors (shown in the inset of Fig. 1(a)) confirm the phase purity of Li_2AGeO_4. All the observed patterns that matched well with the standard JCPDS PDF No. 24-0675 for Li_2ZnGeO_4 and JCPDS No. 24-0627 for Li_2MgGeO_4 ceramics were successfully indexed with no secondary phase peaks detected, which indicates that both compounds crystallized in an orthorhombic olivine structure with a space group $Pmn2_1$. The refined unit cell volumes of the ceramics sintered at different temperatures are shown in Fig. 1(c). Obviously, with increasing sintering temperature, the unit cell volume decreased monotonously. This suggests that the distances between the ions were shortened and the crystal structure of Li_2AGeO_4 (A = Zn, Mg) were compressed with increasing sintering temperature. In addition, it is evidence that Li_2ZnGeO_4 (175.14 $Å^3$) has a larger unit cell than Li_2MgGeO_4 (174.98 $Å^3$), which can be explained by the larger ionic radius of Zn^{2+} (0.74 Å) than Mg^{2+} (0.72 Å). The theoretical densities were calculated based on the refined unit cell volume and atomic weight and yielded 4.08 g/cm^3 for Li_2ZnGeO_4 and 3.31 g/cm^3 for Li_2MgGeO_4. A schematic crystal structure of the Li_2AGeO_4 (A = Zn, Mg) is presented in Fig. 1(d). Li and Ge cations occupy the tetrahedral sites, with the neighboring [LiO_4] and [GeO_4] corner connected. The A cations (Zn or Mg) are coordinated by 6 oxygens to form [AO_6] octahedra and all the octahedra are corner shared with the adjacent tetrahedra.

SEM images of the polished and thermally etched surfaces of the best-sintered samples are shown in the inset of Fig. 2. A dense and

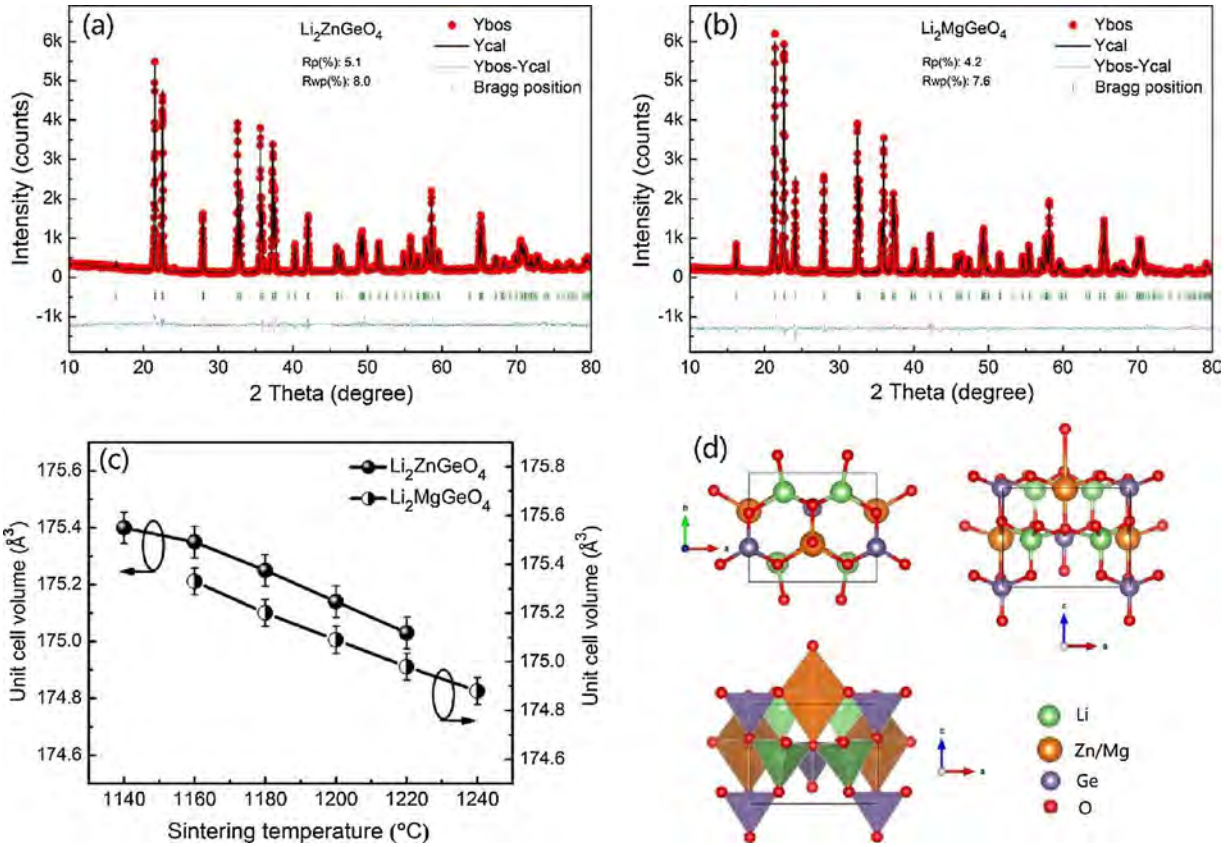

Fig. 1. Rietveld refinement of the room temperature XRD data for the (a) Li_2ZnGeO_4 and (b) Li_2MgGeO_4 ceramic, (c) unit cell volume of Li_2AGeO_4 ceramics as a function of temperature, and schematic crystal structure of the Li_2AGeO_4 (A = Zn, Mg) ceramics.

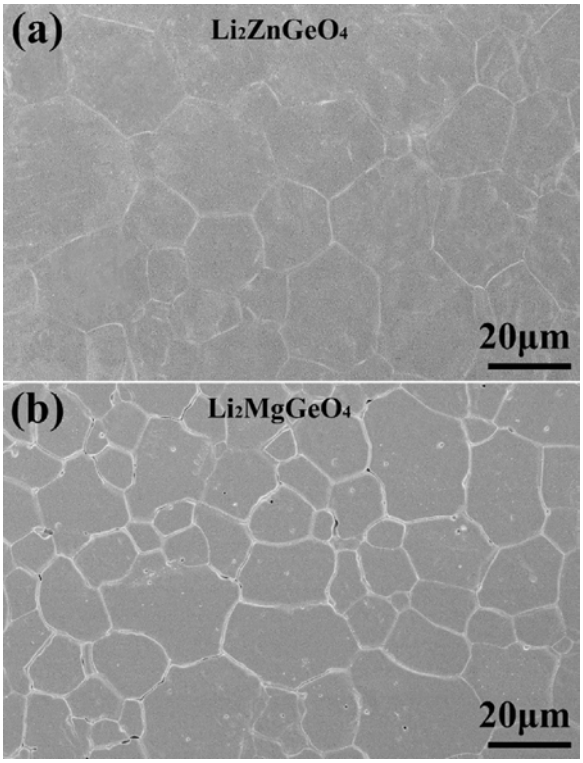

Fig. 2. SEM images of the polished and thermally etched surfaces of the Li_2AGeO_4 (A = Zn, Mg) ceramics sintered at optimum temperature.

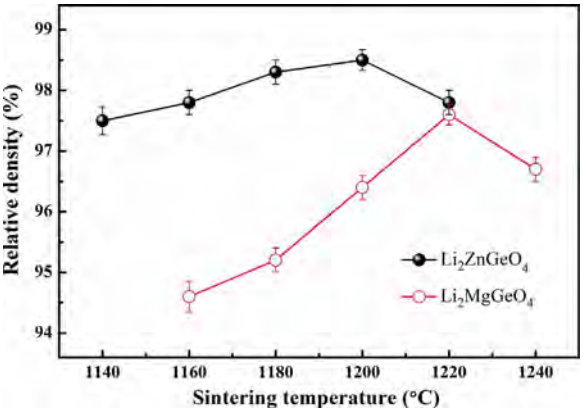

Fig. 3. The relative density of the Li_2AGeO_4 (A = Zn, Mg) ceramics as a function of temperature.

homogeneous microstructure with clear grain boundary is observed for both samples. The average grain size is 15 ~ 25 μm for Li_2ZnGeO_4 and 10 ~ 20 μm for Li_2MgGeO_4 ceramics, respectively. The variation in relative densities of the Li_2AGeO_4 (A = Zn, Mg) ceramics as a function of temperature is shown in Fig. 3. As the sintering temperatures increased, the relative density increased and obtained a saturated value, followed by a slight decrease in higher temperatures. The highest value ~ 98.5% of the theoretical density (~4.08 g/cm^3) was obtained for Li_2ZnGeO_4 ceramic sintered at 1200 °C and ~ 97.6% for Li_2MgGeO_4 ceramic at 1220 °C. By comparison, the densification sintering temperature of the Li_2ZnGeO_4 is slightly lower than Li_2MgGeO_4 ceramic, but the relative density is higher than Li_2MgGeO_4 ceramic.

Microwave dielectric properties (ε_r, $Q \times f$, and τ_f) of the Li_2AGeO_4 (A = Zn, Mg) ceramics sintered at different temperatures are presented in Fig. 4. Over the sintering temperature range 1140–1220 °C, the relative permittivity of Li_2ZnGeO_4 ceramics varied slightly and fluctuated around 6.5. The ε_r of Li_2MgGeO_4 ceramics exhibited similar variation tendency to that of Li_2ZnGeO_4 ceramics. A maximum ε_r value 6.1 was achieved when sintered at 1220 °C for Li_2MgGeO_4, which was slightly lower than Li_2ZnGeO_4. The difference in relative permittivity could be explained by the lower ionic polarization of $\alpha(Mg^{2+})$ (1.32 Å^3) than $\alpha(Zn^{2+})$ (2.04 Å^3) based on the Clausius-Mosotti equation [24]. The calculated theoretical permittivity of Li_2ZnGeO_4 is 7.2 and 6.1 for Li_2MgGeO_4.

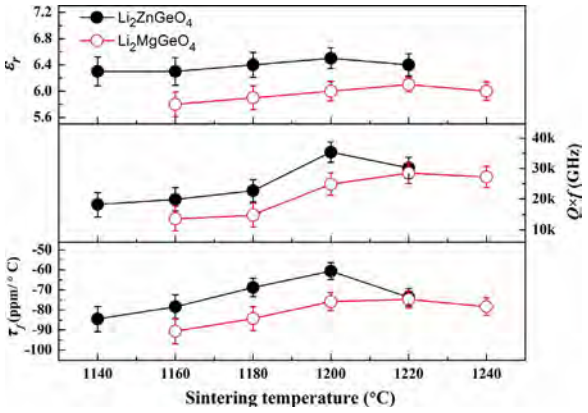

Fig. 4. The microwave dielectric permittivity, $Q \times f$ and τ_f value of the Li_2AGeO_4 (A = Zn, Mg) ceramics as a function of temperature.

It is well known that at microwave frequency region the dielectric loss could be influenced by many factors that can be classified into two categories: the intrinsic factors related to the inharmonic lattice vibration and the extrinsic ones, e.g. density, grain boundary, pores, secondary phase, etc [25,26]. Obviously, $Q \times f$ values of Li_2AGeO_4 (A = Zn, Mg) ceramics exhibit similar variation trend to the corresponding relative densities. The result suggests that in the present work, the bulk density plays prominent roles in controlling the dielectric loss. Optimal $Q \times f$ values of 35,400 GHz and 28,500 GHz for Li_2ZnGeO_4 and Li_2MgGeO_4 ceramics were obtained at their relative densification temperatures (1200 °C and 1220 °C, respectively). Similarly, the temperature coefficient of the resonance frequency of Li_2AGeO_4 (A = Zn, Mg) ceramics of varied slightly and fluctuated with the sintering temperature. The τ_f values of –60.6 ppm/°C for Li_2MgGeO_4 and –74.7 ppm/°C for Li_2MgGeO_4 were obtained. Unfortunately, the large negative τ_f values are unacceptable for practical applications where a near-zero τ_f value is expected. In order to adjust the thermal stability of Li_2AGeO_4 ceramics, an effective and successful strategy of an addition of another phase with opposite τ_f value to form composite ceramics is utilized [27,28]. In the present work, $CaTiO_3$ with a positive τ_f of +800 ppm/°C was chosen as the τ_f adjustor.

Fig. 5 shows the XRD patterns of (1-x)Li_2AGeO_4-$x$$CaTiO_3$ (A = Zn, Mg) ceramics. Only the peaks of $CaTiO_3$ (JCPDS No. 76-2400) and Li_2AGeO_4 phase were observed. This reveals that no chemical reaction occurred between Li_2AGeO_4 (A = Zn, Mg) and $CaTiO_3$ and they could co-exist in the (1-x)Li_2AGeO_4-$x$$CaTiO_3$ (A = Zn, Mg) system.

Fig.6 shows the ε_r, $Q \times f$, and τ_f values of (1-x)Li_2AGeO_4-$x$$CaTiO_3$ (A = Zn, Mg) ceramics as a function of volume fraction of $CaTiO_3$. As shown, the ε_r values of (1-x)Li_2AGeO_4-$x$$CaTiO_3$ (A = Zn, Mg) ceramics increased with increasing $CaTiO_3$ content, attributed to the higher ε_r value of $CaTiO_3$ (~170). However, $CaTiO_3$ addition to Li_2AGeO_4 (A = Zn, Mg) is detrimental to the $Q \times f$ value. As well known, the quality factor is sensitive to the extrinsic effects, especially the

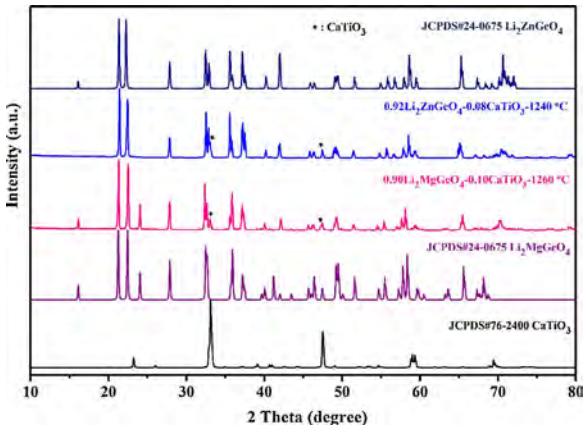

Fig. 5. XRD patterns of (a) $0.92Li_2ZnGeO_4$-$0.08CaTiO_3$ ceramics sintered at 1240 °C, and (b) the $0.90Li_2MgGeO_4$-$0.10CaTiO_3$ ceramics sintered at 1260 °C.

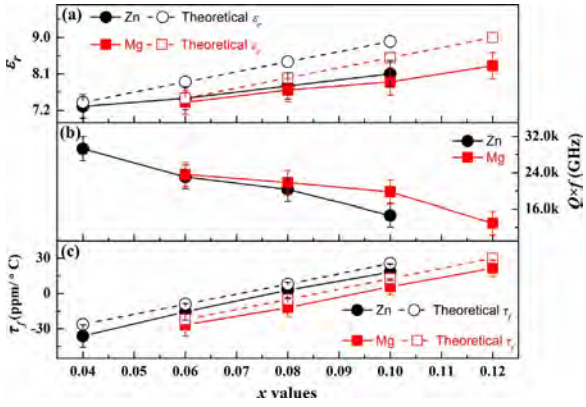

Fig. 6. The ε_r, theoretical ε_r, $Q \times f$, τ_f, and theoretical τ_f values of $(1\text{-}x)Li_2AGeO_4$-$xCaTiO_3$ (A = Zn, Mg) ceramics as a function of the x values.

secondary phases. The $CaTiO_3$ addition as the second phase could deteriorate the $Q \times f$ values. Importantly, the τ_f values of $(1\text{-}x)Li_2AGeO_4$-$xCaTiO_3$ ceramics increased with the x values, showing a shift from negative to positive. As expected, a near-zero τ_f value of +2.9 ppm/°C was obtained in $0.92Li_2ZnGeO_4$-$0.08CaTiO_3$ composite when sintered at 1240 °C and +5.8 ppm/°C for $0.90Li_2MgGeO_4$-$0.10CaTiO_3$ composite sintered at 1260 °C. According to the empirical Lichtenecker logarithmic rule for a two-phase composite, the theoretical ε_r and τ_f values can be described by the following equations [29]:

$$\lg\varepsilon = x_1 \lg\varepsilon_1 + x_2 \lg\varepsilon_2 \quad (1)$$

$$\tau_f = x_1\tau_{f1} + {}_2\tau_{f2} \quad (2)$$

where x_1 and x_2 are the volume fractions, ε_1 and ε_2 are the permittivities, τ_{f1} and τ_{f2} are the τ_f values of the pure Li_2AGeO_4 (A = Zn, Mg) and $CaTiO_3$ phase, respectively. The theoretical ε_r and τ_f values of Li_2AGeO_4-$CaTiO_3$ are calculated using the equations and shown in Fig. 6. By comparison, the measured ε_r and τ_f values were closed to the theoretical values.

Table 1 lists the sintering temperature and microwave dielectric properties of some low-permittivity microwave dielectric ceramics in the A_2BO_4 system. By comparison, the relative permittivity of the Li_2AGeO_4 (A = Zn, Mg) ceramics is close to that of the Zn_2MO_4 (M = Si, Ge). The quality factors of Li_2AGeO_4 are inferior compared with Zn_2MO_4 (M = Si, Ge), however, superior to Li_2MgSiO_4. Especially, it is worth noting that the Li-containing ceramics exhibited much lower sintering temperatures than others. Furthermore, all the listed A_2BO_4 microwave dielectric ceramics possess negative τ_f values. The successful thermal compensation in Li_2AGeO_4 (A = Zn, Mg) ceramics makes them possible candidates for practical applications.

4. Conclusions

Orthorhombic olivine structure Li_2AGeO_4 (A = Zn, Mg) ceramics were formed via the solid-state reaction method. The densification sintering temperature of the Li_2ZnGeO_4 ceramic is 1200 °C with relative density 98.5%, and at the same temperature to achieve the best microwave dielectric performances with $\varepsilon_r \sim 6.5$, $Q \times f \sim 35{,}400$ GHz, and $\tau_f \sim -60.6$ ppm/°C. The Li_2MgGeO_4 ceramic sintered at 1220 °C for 6 h exhibited high relative density with 97.6% and excellent microwave dielectric properties with $\varepsilon_r \sim 6.1$, $Q \times f \sim 28{,}500$ GHz, and $\tau_f \sim -74.7$ ppm/°C. Furthermore, the large negative τ_f values of Li_2AGeO_4 (A = Zn, Mg) ceramics could be compensated by forming composite ceramics with $CaTiO_3$.

Acknowledgments

This work was supported by Natural Science Foundation of China (Nos. 51502047, 21561008, and 21761008), the Natural Science Foundation of Guangxi Zhuang Autonomous Region (Nos. 2015GXNSFFA139003, 2016GXNSFBA380134, and 2016GXNSFAA380018), Project of Scientific Research and Technical Exploitation Program of Guilin (2016010702-2 and 20170225), and Innovation Project of Guangxi Graduate Education (YCBZ2017052). Chunchun Li gratefully acknowledges the Guangxi Scholarship Fund of Guangxi Education Department.

Table 1
Microwave dielectric properties of the olivine structure ceramics.

Ceramics	S.T. (°C)	ε_r	$Q \times f$ (GHz)	τ_f (ppm/°C)	Reference
Mg_2SiO_4	1550	7.5	114,730	–59	[13]
Zn_2SiO_4	1325	6.6	198,400	–41.6	[14]
Mg_2GeO_4	1450	5.48	11,037	–27.61	[19]
Zn_2GeO_4	1300	6.87	102,700	–32.4	[20]
Mg_2SnO_4	1600	8.41	55,100	−62	[30]
$(Mg_{0.95}Ni_{0.05})_2SnO_4$	1550	8.72	103,100	−62.8	[31]
Li_2MgSiO_4	1250	5.1	15,380	–	[32]
Li_2MgGeO_4	1220	6.1(± 0.3)	28,500(± 200)	–74.7(± 4)	This work
Li_2ZnGeO_4	1200	6.5(± 0.3)	35,400(± 300)	–60.6(± 3)	This work
0.92 LZG-0.08 CT	1240	7.8(± 0.4)	20,300(± 200)	+2.9(± 0.1)	This work
0.90 LMG-0.10 CT	1260	7.9(± 0.4)	19,760(± 200)	+5.8(± 0.3)	This work

References

[1] Z.Y. Zou, Z.H. Chen, X.K. Lan, W.Z. Lu, B. Lua, B. Ullah, X.H. Wang, W. Lei, Weak ferroelectricity and low-permittivity microwave dielectric properties of $Ba_2Zn_{(1+x)}Si_2O_{(7+x)}$ ceramics, J. Eur. Ceram. Soc. 37 (2017) 3065–3071.

[2] H.Z. Zuo, X.L. Tang, H.W. Zhang, Y.M. Lai, Y.L. Jing, H. Su, Low-dielectric-constant $LiAlO_2$ ceramics combined with LBSCA glass for LTCC applications, Ceram. Int. 43 (2017) 8951–8955.

[3] W. Luo, J. Guo, C. Randall, M. Lanagan, Effect of porosity and microstructure on the microwave dielectric properties of rutile, Mater. Lett. 200 (2017) 101–104.

[4] Y. Huang, J. Yu, C. Shen, M. Tang, Microstructure and microwave dielectric properties of $(1-x)MgAl_2O_4$–$x(Ca_{0.8}Sr_{0.2})TiO_3$ ceramics, J. Electron. Mater. 45 (2016) 4903–4907.

[5] P. Wang, Y.R. Wang, J.X. Bi, H.T. Wu, Effects of Zn^{2+} substitution on the crystal structure, Raman spectra, bond energy and microwave dielectric properties of Li_2MgTiO_4 ceramics, J. Alloys Compd. 721 (2017) 143–148.

[6] C.X. Hu, Y. Liu, P. Liu, B. Yang, Novel low loss, low permittivity $(1-x)SiO_2 - xTiO_2$ + ywt% H_3BO_3 microwave dielectric ceramics for LTCC applications, J. Alloys Compd. 712 (2017) 804–810.

[7] A. Ullah, H.X. Liu, H. Hao, J. Iqbal, Z.H. Yao, M.H. Cao, Influence of TiO_2 additive on sintering temperature and microwave dielectric properties of $Mg_{0.90}Ni_{0.1}SiO_3$ ceramics, J. Eur. Ceram. Soc. 37 (2017) 3045–3049.

[8] J.A. Montoya, P. Angel, T. Viveros, The effect of temperature on the structural and textural evolution of sol–gel Al_2O_3–TiO_2 mixed oxides, J. Mater. Chem. 11 (2001) 944–950.

[9] K.P. Surendran, P.V. Bijumon, P. Mohanan, M.T. Sebastian, (1-x)$MgAl_2O_4$-xTiO_2 dielectrics for microwave and millimeter wave applications, Appl. Phys. A 81 (2005) 823–826.

[10] W. Lei, W.Z. Lu, X.C. Wang, Temperature compensating $ZnAl_2O_4$–Co_2TiO_4 spinel-based low-permittivity microwave dielectric ceramics, Ceram. Int. 38 (2012) 99–103.

[11] W. Lei, W.Z. Lu, D. Liu, J.H. Zhu, Phase evolution and microwave dielectric properties of (1-*x*)$ZnAl_2O_4$-xMg_2TiO_4 ceramics, J. Am. Ceram. Soc. 92 (2009) 105–109.

[12] G. Dou, D.X. Zhou, M. Guo, S.P. Gong, Y.X. Hu, Low-temperature sintered Mg_2SiO_4–$CaTiO_3$ ceramics with near-zero temperature coefficient of resonant frequency, J. Mater. Sci. 24 (2013) 1431–1438.

[13] K.X. Song, X.M. Chen, X.C. Fan, Effect of Mg/Si ratio on microwave dielectric characteristics of forsterite ceramics, J. Am. Ceram. Soc. 90 (2007) 1808–1811.

[14] M.Z. Dong, Z.X. Yue, H. Zhuang, S.P. Meng, L.T. Li, Microstructure and microwave dielectric properties of TiO_2-doped Zn_2SiO_4 ceramics synthesized through the sol–gel process, J. Am. Ceram. Soc. 91 (2008) 3981–3985.

[15] I. Koseva, V. Nikolov, N. Petrova, P. Tzvetkov, M. Marychev, Thermal behavior of germanates with olivine structure, Thermochim. Acta 646 (2016) 1–7.

[16] N. Nakayama, K. Takahashi, K. Fujiwara, A. Nakatsuka, M. Isobe, Y. Ueda, Structural phase transitions of Li_2MgSiO_4 and Li_2MgGeO_4, Trans. Mat. Res. Soc. Jpn. 38 (2013) 419–422.

[17] R.L. Millard, R.C. Peterson, B.K. Hunter, Study of the cubic to tetragonal transition in Mg_2TiO_4 and Zn_2TiO_4 spinels by ^{17}O MAS NMR and rietveld refinement of X-ray diffraction data, Am. Mineral. 80 (1995) 885–896.

[18] N.L. Ross, A. Navrotsky, The Mg_2GeO_4 olivine-spinel phase transition, Phys. Chem. Min. 14 (1987) 473–481.

[19] C.X. Chen, S.P. Wu, Y.X. Fan, Synthesis and microwave dielectric properties of B_2O_3-doped Mg_2GeO_4 ceramics, J. Alloys Compd. 578 (2013) 153–156.

[20] S.P. Wu, Q. Ma, Synthesis, characterization and microwave dielectric properties of Zn_2GeO_4 ceramics, J. Alloys Compd. 567 (2013) 40–46.

[21] H.F. Zhou, J.Z. Gong, N. Wang, X.L. Chen, A novel temperature stable microwave dielectric ceramic with low sintering temperature and high quality factor, Ceram. Int. 42 (2016) 8822–8825.

[22] G. Sumesh, S.M. Thomas, Synthesis and microwave dielectric properties of novel temperature stable high Q, $Li_2ATi_3O_8$ (A = Mg, Zn) ceramics, J. Am. Ceram. Soc. 93 (2010) 2164–2166.

[23] H.C. Xiang, L. Fang, W.S. Fang, Y. Tang, C.C. Li, A novel low-firing microwave dielectric ceramic $Li_2ZnGe_3O_8$ with cubic spinel structure, J. Eur. Ceram. Soc. 37 (2017) 625–629.

[24] S. Roberts, Dielectric constants and polarizabilities of ions in simple crystals and barium titanate, Phys. Rev. 76 (1949) 1215–1220.

[25] J. Li, L. Fang, H. Luo, J. Khaliq, Y. Tang, C.C. Li, Li_4WO_5: a temperature stable low-firing microwave dielectric ceramic with rock salt structure, J. Eur. Ceram. Soc. 36 (2016) 243–246.

[26] S.H. Yoon, D.W. Kim, S.Y. Cho, H.K. Sun, Investigation of the relations between structure and microwave dielectric properties of divalent metal tungstate compounds, J. Eur. Ceram. Soc. 26 (2006) 2051–2054.

[27] W. Lei, W.Z. Lu, J.H. Zhu, X.H. Wang, Microwave dielectric properties of $ZnAl_2O_4$-TiO_2 spinel-based composites, Mater. Lett. 61 (2007) 4066–4069.

[28] Y. Wu, D. Zhou, J. Guo, L.X. Pang, H. Wang, X. Yao, Temperature stable microwave dielectric ceramic $0.3Li_2TiO_3$-$0.7Li(Zn_{0.5}Ti_{1.5})O_4$ with ultra-low dielectric loss, Mater. Lett. 65 (2011) 2680–2682.

[29] T. Takada, S.F. Wang, S. Yoshikawa, S.J. Jang, R.E. Newnham, Effect of glassadditions on BaO–TiO_2–WO_3 microwave ceramics, J. Am. Ceram. Soc. 77 (1994) 1909–1916.

[30] Y.C. Chen, Y.N. Wang, C.H. Hsu, Elucidating the dielectric properties of Mg_2SnO_4 ceramics at microwave frequency, J. Alloys Compd. 509 (2011) 9650–9653.

[31] Y.C. Chen, Y.N. Wang, C.H. Hsu, Enhancement microwave dielectric properties of Mg_2SnO_4 ceramics by substituting Mg^{2+} with Ni^{2+}, Mater. Chem. Phys. 133 (2012) 829–833.

[32] S. George, P.S. Anjana, V.N. Deepu, P. Mohanan, M.T. Sebastian, Low-temperature sintering and microwave dielectric properties of Li_2MgSiO_4 ceramics, J. Am. Ceram. Soc. 92 (2009) 11244–11249.